Published in final edited form as:
Neuron. 2009 February 12; 61(3): 425–438. doi:10.1016/j.neuron.2008.12.015.

Activity-Dependent Modulation of Limbic Dopamine D3 Receptors by CaMKII

Xian-Yu Liu[1,7], **Li-Min Mao**[1,7], **Guo-Chi Zhang**[1], **Christopher J. Papasian**[1], **Eugene E. Fibuch**[2], **Hong-Xiang Lan**[4], **Hui-Fang Zhou**[5], **Ming Xu**[6,*], and **John Q. Wang**[1,2,3,*]

1 *Department of Basic Medical Science, University of Missouri-Kansas City, Kansas City, MO 64108, USA*

2 *Department of Anesthesiology, School of Medicine, University of Missouri-Kansas City, Kansas City, MO 64108, USA*

3 *Department of Pharmacology, School of Pharmacy, University of Missouri-Kansas City, Kansas City, MO 64108, USA*

4 *Department of Behavioral Neuroscience, Oregon Health and Science Center, Portland, Oregon 97239, USA*

5 *Department of Anesthesiology, Washington University School of Medicine, St. Louis, MO 63110, USA*

6 *Department of Anesthesia and Critical Care, The University of Chicago, Chicago, IL 60637, USA*

Summary

Ca^{2+}/calmodulin-dependent protein kinase II (CaMKII) is central to synaptic transmission. Here we show that synaptic CaMKIIα binds to the third intracellular loop of the limbic dopamine D3 receptor (D3R). This binding is Ca^{2+}-sensitive and is sustained by autophosphorylation of CaMKII, providing an unrecognized route for the Ca^{2+}-mediated regulation of D3Rs. The interaction of CaMKIIα with D3Rs transforms D3Rs into a biochemical substrate of the kinase and promotes the kinase to phosphorylate D3Rs at a selective serine site (S229). In accumbal neurons *in vivo*, CaMKIIα is recruited to D3Rs by rising Ca^{2+} to increase the CaMKIIα-mediated phosphorylation of D3Rs, thereby transiently inhibiting D3R efficacy. Notably, the D3R inhibition is critical for integrating dopamine signaling to control behavioral sensitivity to the psychostimulant cocaine. Our data identify CaMKIIα as a recruitable regulator of dopamine receptor function. By binding and phosphorylating limbic D3Rs, CaMKIIα modulates dopamine signaling and psychomotor function in an activity-dependent manner.

Keywords

striatum; nucleus accumbens; calcium; calmodulin; adenylyl cyclase; cAMP; CREB; locomotion; cocaine

*Corresponding author: Dr. John Q. Wang, Department of Basic Medical Science, University of Missouri-Kansas City, School of Medicine, 2411 Holmes Street, Kansas City, Missouri 64108, USA, Tel: (816) 235-1786; Fax: (816) 235-5574, E-mail: wangjq@umkc.edu.
[7]Equal contributors

Introduction

Dopamine is a major neurotransmitter in the mammalian brain. This transmitter exerts its pleiotropic actions through interactions with two classes of dopamine receptors: the D1 class (D1 and D5 subtypes) and the D2 class (D2, D3, and D4 subtypes). The former is coupled to Gαs-proteins, whereas the latter is generally coupled to Gαi/o-proteins. Through Gαi/o-proteins, the D2 class of receptors inhibits adenylyl cyclase and the downstream formation of cAMP (Neve et al., 2004). Remarkably, among all dopamine receptor subtypes, the dopamine D3 receptor (D3R), one of the lesser-investigated subtypes, shows a unique distribution pattern in the forebrain. D3Rs are preferentially expressed in the mesolimbic dopaminergic projection areas, including the nucleus accumbens (NAc) (Sokoloff et al., 1990; Bouthenet et al., 1991). This specific localization of D3Rs suggests a significant role of the receptor in the control of reward, motivation, cognition, emotion, and extrapyramidal motor functions. Moreover, malfunction of D3Rs has been frequently associated with the pathogenesis of various mental illnesses such as schizophrenia, depression, and substance addiction (reviewed in Heidbreder et al., 2005; Sokoloff et al., 2006; Richtand, 2006).

Ca^{2+}/calmodulin-dependent protein kinase II (CaMKII) is an enzyme that is abundant in brain cells, especially at synaptic sites (Kelly et al., 1984). The enzyme is removed from its autoinhibitory state and activated by the binding of Ca^{2+} and calmodulin (CaM). Activated CaMKII accesses and phosphorylates not only exogenous substrates but also its own autophosphorylation site (T286 in the α isoform) within the autoregulatory domain. The autophosphorylation renders a Ca^{2+}/CaM-independent (autonomous) kinase activity even after the initial Ca^{2+} stimulus subsides (Hudmon and Schulman, 2002; Colbran and Brown, 2004; Griffith, 2004). As such, CaMKII integrates and prolongs the information conveyed by diverse forms of Ca^{2+} transients and serves as a dynamic regulator that decodes activity-dependent Ca^{2+} signals into various forms of synaptic activity and plasticity (reviewed in Hudmon and Schulman, 2002; Lisman et al., 2002; Colbran and Brown, 2004).

The multifunctional nature of CaMKII also stems from its interactions with various binding partners in defined subcellular regions (Colbran, 2004). Through direct protein-protein interactions, CaMKII vigorously regulates expression and function of interacting partners and vice versa. In searching for new targets of CaMKII at synaptic sites, we identify the limbic D3R as a direct substrate of CaMKII. We show that CaMKIIα interacts directly with the N-terminal region of the third intracellular loop of D3Rs in a Ca^{2+}- and autophosphorylation-sensitive manner *in vitro*. This interaction allows CaMKII to phosphorylate D3Rs at a selective serine residue. In accumbal neurons *in vivo*, Ca^{2+} stimulates the association of CaMKII with D3Rs and increases serine phosphorylation of D3Rs, resulting in suppression of D3R function. The CaMKII-mediated inhibition of D3Rs plays a significant role in regulating behavioral responsiveness to cocaine. Collectively, our results demonstrate a new synaptic model for the activity-dependent regulation of limbic D3Rs by CaMKII.

Results

CaMKIIα directly binds to D3Rs *in vitro*

D3Rs contain a large third intracellular domain that is a main site for protein-protein interactions (Fig. S1). To search for new proteins that bind to this domain, we prepared glutathione-S-transferase (GST)-fusion proteins containing the second or third intracellular loop of rat D3Rs, $D3R_{IL2}$ or $D3R_{IL3}$ (Fig. 1A), and used them as immobilized (GST-bound) baits to screen NAc lysates in pull-down assays. We found a protein (~50 kDa) that was specifically precipitated by GST-$D3R_{IL3}$, but not by GST alone (Fig. 1B) or GST-$D3R_{IL2}$ (data not shown). This protein was subsequently identified as CaMKIIα by mass spectrometry. Immunoblot analysis confirmed that GST-$D3R_{IL3}$, but not GST-$D3R_{IL2}$ or GST alone,

precipitated CaMKIIα (Fig. 1C). Neither the GST-fusion proteins nor GST precipitated CaMKIV, another isoform of CaMK (Fig. 1C). This indicates the selectivity of D3Rs in the interaction with CaMKII. To identify the specific CaMKIIα region responsible for the interaction with D3Rs, GST-fusion proteins were prepared from three major structures of CaMKIIα: the N-terminal catalytic domain (GST-CaMKIIα_{CD}), the regulatory domain (GST-CaMKIIα_{RD}), and the C-terminal association domain (GST-CaMKIIα_{AD}) (Fig. 1D). We found that GST-CaMKIIα_{CD} precipitated D3Rs in accumbal lysates, whereas GST-CaMKIIα_{RD}, GST-CaMKIIα_{AD}, and GST-CaMKIV did not (Fig. 1E). None of the GST-fusion proteins precipitated dopamine D1 receptors (D1Rs) (Fig. 1F). Thus, the primary CaMKIIα region for the interaction with D3Rs is restricted to CaMKIIα_{CD}. All blots were probed in parallel with a GST antibody to ensure equivalent protein loading (data not shown).

To define whether the CaMKIIα-D3R interaction is direct, and to reveal the accurate region of $D3R_{IL3}$ involved in the interaction, we conducted *in vitro* binding assays with purified proteins (Fig. 1G-J). We found that CaMKIIα bound to immobilized GST-$D3R_{IL3}$ and GST-$D3R_{IL3}$(R210-P239), but not to other GST-$D3R_{IL3}$ fragments (Fig. 1H). No CaMKIIα bound to GST-$D2R_{IL3}$(I210-V270) (Fig. 1I). In the reverse experiment, $D3R_{IL3}$ bound to immobilized GST-CaMKIIα and GST-CaMKIIα_{CD}, but not to GST-CaMKIIα_{RD}, GST-CaMKIIα_{AD}, and GST-CaMKIV (Fig. 1J). These results demonstrate that CaMKIIα directly binds to D3Rs *in vitro*. The R210-P239 fragment, a 30-amino acid region at the N-terminus of $D3R_{IL3}$, contains a site critical for binding to the catalytic domain of CaMKIIα.

Ca^{2+} enhances the binding of CaMKIIα to D3Rs

Binding of Ca^{2+}/CaM to the regulatory domain of CaMKII is an essential step for releasing autoinhibition and activating the enzyme. Thus, Ca^{2+} usually regulates the binding properties of CaMKII (Bayer et al., 2001; Colbran et al., 2004). To determine if Ca^{2+} affects the CaMKIIα association with D3Rs, we tested the capacity of CaMKIIα to bind to GST-$D3R_{IL3}$ in the presence of Ca^{2+}, CaM, or both. Similar to the results from the above *in vitro* binding assays performed in the absence of exogenously added Ca^{2+}/CaM, CaMKIIα showed a low level of constitutive binding to GST-$D3R_{IL3}$ (L1 in Fig. 2A). Interestingly, the addition of Ca^{2+} (0.5 mM) and CaM (1 μM) together, but not Ca^{2+} or CaM alone, significantly increased the amount of CaMKIIα bound to $D3R_{IL3}$ (L4 vs. L2 and L3 in Fig. 2A and 2B). This increase was prevented by adding the Ca^{2+} chelator EGTA at 1 mM (L5 in Fig. 2A), and could occur to CaMKIIα that was not autophosphorylated at T286 as evidenced by the fact that no T286-autophosphorylated CaMKIIα (pCaMKIIα) was detected in these binding assays with a phospho-specific antibody due to the absence of ATP throughout the reaction (the middle panel of Fig. 2A). These results demonstrate that activation of CaMKIIα by Ca^{2+}/CaM was sufficient to enhance its affinity for D3Rs. Consistent with this, an increase in the CaMKIIα-$D3R_{IL3}$ binding was observed only with the wild-type (WT) CaMKIIα, but not with the Ca^{2+}/CaM binding-defective CaMKIIα mutant T305/306D (Fig. 2C and 2D) (Colbran and Soderling, 1990). Moreover, a peptide fragment (L290-A309), that corresponds to the CaM-binding domain of CaMKII and thereby antagonizes the CaM-CaMKII binding, blocked the Ca^{2+}/CaM-induced enhancement of the CaMKIIα binding to D3Rs (Fig. 2E). To determine if CaM itself binds to $D3R_{IL3}$, we conducted *in vitro* binding assays with purified CaM. No binding of CaM to GST-$D3R_{IL3}$ or GST was observed, whereas CaM bound to GST-CaMKIIα in a Ca^{2+}-dependent fashion (Fig. 2F).

Autophosphorylation of CaMKIIα further enhances the binding of CaMKIIα to D3Rs

Activation of CaMKIIα by Ca^{2+}/CaM results in autophosphorylation at T286 in the regulatory domain of adjacent CaMKIIα subunits, which 'traps' CaM and keeps the enzyme in a catalytically active conformation, an autonomous (Ca^{2+}/CaM-independent) activity, even after the initial Ca^{2+}/CaM signal subsides (Meyer et al., 1992). A series of experiments was carried

out to determine the influence of T286 autophosphorylation on the CaMKIIα-D3R binding. The unphosphorylated WT kinase exhibited constitutive and enhanced binding to $D3R_{IL3}$ in the absence and presence of Ca^{2+}/CaM, respectively (Fig. 3A). Interestingly, WT CaMKIIα, that was activated by Ca^{2+}/CaM and autophosphorylated at T286 prior to the binding assays, showed a further enhanced level of binding (L3 and L4 in Fig. 3A) as compared to unphosphorylated WT, regardless of the presence or absence of Ca^{2+}/CaM in the binding assays (Fig. 3A and 3D). An autophosphorylation-defective mutant, T286A, showed the same level of binding to D3Rs in the presence or absence of ATP (Fig. 3B and 3D). In contrast, a constitutively active (Ca^{2+}/CaM-independent) mutant, T286D that shares the property of autophosphorylated CaMKIIα, showed a high level of binding to D3Rs, which was not affected by the addition of Ca^{2+}/CaM or Ca^{2+}/CaM/ATP (Fig. 3C and 3D). These data indicate that, while the basal (unstimulated) and Ca^{2+}/CaM-stimulated binding to D3Rs requires no autophosphorylation, autophosphorylation of T286 further increases the capacity of CaMKIIα to bind to D3Rs.

The binding properties of autophosphorylated CaMKIIα were further analyzed in binding assays with EGTA (1 mM) added at different times. As before, an increased amount of $D3R_{IL3}$-bound CaMKIIα was detected when Ca^{2+}/CaM and ATP were added for 20 min (L3 in Fig. 3E). The addition of EGTA substantially inhibited the CaMKIIα binding. However, this inhibition occurred only when EGTA was added in the early phase (< 2 min, L4-L6 in Fig. 3E). When the binding reaction lasted long enough (2–15 min), EGTA was no longer effective (L7 and L8 in Fig. 3E). The $D3R_{IL3}$-bound enzyme from the ATP-containing assays was autophosphorylated at T286, and the level of this autophosphorylation paralleled well with the capacity of the enzyme in binding to D3Rs at different EGTA-adding times (Fig. 3E). These data suggest that the CaMKIIα binding to D3Rs and T286-autophosphorylation are initially reversible, but become Ca^{2+}/CaM-independent when the kinase transforms to an autonomous state.

Like the unphosphorylated enzyme, autophosphorylated CaMKIIα bound to the same N-terminal region (R210-P239) of $D3R_{IL3}$ (Fig. 3F). This region was therefore further analyzed to identify a sufficient binding motif. A panel of peptides derived from this region was used to compete with the R210-P239 fragment for binding to CaMKIIα. It was found that four out of six peptides (P1, P2, P3, and P5) blocked the binding of GST-$D3R_{IL3}$(R210-P239) to active CaMKIIα (Fig. S2A) or autophosphorylated CaMKIIα (Fig. 3G). These four peptides, when used in a biotinylated form, pulled down CaMKIIα (Fig. S2B). Thus, a 14-residue motif (RILTRQNSQCISIR) contained by all four peptides constitutes a core motif for CaMKIIα binding. Notably, this motif is highly conserved among mammals.

CaMKII phosphorylates S229 in $D3R_{IL3}$

A comparison of the amino acid sequences revealed a remarkable homology between the CaMKIIα-binding region in $D3R_{IL3}$ and the sequences spanning a T286 pseudosubstrate region in CaMKIIα (Yang and Schulman, 1999), S1303 in NR2B (Strack et al., 2000), and an S/T site in two classical CaMKII substrates, autocamtide-2 and syntide-2 (Fig. 4A). This suggested that $D3R_{IL3}$ might serve as a phosphorylation substrate of CaMKII. Indeed, CaMKIIα phosphorylated GST-$D3R_{IL3}$, but not GST, in the presence of Ca^{2+}/CaM (Fig. 4B). Similarly, CaMKIIα phosphorylated the GST-$D3R_{IL3}$(R210-P239) fragment (Fig. 4C). This phosphorylation was rapid (Fig. 4D) and comparable to the phosphorylation of an NR2B fragment (Fig. S3A). The kinetic parameter, *Km*, was notably low, 65.9 ± 1.2 nM (Fig. 4E), suggesting that $D3R_{IL3}$ like NR2B (Omkumar et al., 1996) acts as a high-affinity substrate. This high-affinity nature implies that phosphorylation of $D3R_{IL3}$ could occur under physiological conditions. In support of this, GST-$D3R_{IL3}$(R210-P239) was phosphorylated at two physiological Ca^{2+} concentrations (Fig. S3B).

To identify accurate phosphorylation site(s) within the R210-P239 fragment, we used a series of synthetic peptides with or without mutations of two known serine sites in this fragment (S229 and S233). Figure 4F shows that the WT S229/233 peptide substrate was phosphorylated by CaMKIIα to a considerable stoichiometry (0.81 mol of phosphate/mol of substrate). Mutation of S233 to Ala (S233A) did not affect the phosphorylation. In contrast, mutation of S229 to Ala (S229A) or S229/233 to Ala (S229/233A) completely abolished the phosphorylation. Thus, S229 rather than S233 or T225 is the site of phosphorylation. The fact that S229 lies within the CaMKII binding motif in $D3R_{IL3}$ and aligns with a phospho-S/T site predicted from the consensus CaMKII phosphorylation sequence, (I/L)*XRXX*(S/T) (White et al., 1998), is noteworthy. The results from tandem mass spectrometry analysis of tryptic digests of CaMKII-phosphorylated GST-$D3R_{IL3}$ conclusively identified S229 as a phosphorylation site (data not shown).

Although the CaMKIIα binding domain in $D3R_{IL3}$ aligns with the substrate recognition motif and contains a high affinity phosphorylation site (S229), a classical enzyme-substrate binding mechanism does not appear to be involved in the CaMKIIα binding to $D3R_{IL3}$. This is supported by the finding that syntide-2 (a model peptide substrate for CaMKII) at concentrations up to 400 μM (>30 times the *Km* for phosphorylation; Hashimoto and Soderling, 1987) failed to compete for the CaMKIIα binding to $D3R_{IL3}$ (Fig. S3C).

CaMKIIα interacts with D3Rs *in vivo*

D3Rs are enriched in accumbal neurons. To determine whether native CaMKIIα and D3Rs interact with each other in these neurons, coimmunoprecipitation was performed using the solubilized synaptosomal fraction (P2) from the rat NAc. A clear and specific band of CaMKIIα, but not CaMKIV, was shown in the D3R precipitates (Fig. 5A). No immunoreactivity of other key synaptic proteins, including postsynaptic density (PSD)-93, PSD-95, synapse-associated protein (SAP) 97, and SAP102, was detected in the D3R precipitates (data not shown). In a reverse coimmunoprecipitation assay, a D3R-specific band was seen in the CaMKIIα precipitates (Fig. 5B). CaMKIIα in D3R-expressing neurons of the rat midbrain structures (substantia nigra and ventral tegmental area) and the rat medial mammillary bodies showed no interaction with D3Rs because no coimmunoprecipitation between the two proteins was seen in the P2 fraction from these regions (Fig. 5C and 5D). In the NAc, the coimmunoprecipitation was seen in WT mice, but not in D3R mutant mice (Fig. S4A). Furthermore, the coimmunoprecipitation occurred in the purified PSD fraction of rat accumbal neurons (Fig. S4B). These data indicate a region-specific interaction between CaMKIIα and D3Rs in the NAc *in vivo* and an interaction that can occur in the PSD. Further evidence supporting the interaction of the two proteins *in vivo* was obtained from yeast two-hybrid assays. Using $D3R_{IL3}$ as bait in the yeast two-hybrid system, we found a prominent interaction between $D3R_{IL3}$ and CaMKIIα (Fig. S4C). The strong interaction with CaMKIIα was also seen for the $D3R_{IL3}$(R210-P239), but not $D3R_{IL3}$(Q240-Q375), fragment (Fig. S4C).

To determine whether the CaMKIIα-D3R interaction is subject to the Ca^{2+} regulation as was observed *in vitro*, we tested the interaction in the presence of the Ca^{2+} ionophore, ionomycin, in rat striatal/NAc slices. Ionomycin induced a concentration-dependent increase in the amounts of CaMKIIα and pCaMKIIα (T286) in the D3R precipitates (Fig. 5E). The CaMK inhibitor KN93 (20 μM), which inhibits CaMK by preventing the CaM binding to the enzyme, blocked the ionomycin-induced binding of CaMKIIα (Fig. 5F) and pCaMKIIα (T286) (Fig. S5) to D3Rs. The inactive analog of KN93, KN92, had no effect (Fig. 5F and Fig. S5). Like KN93, the highly selective CaMKII inhibitory peptide Tat-CaMKIINtide (Chang et al., 1998;Vest et al., 2007) at 5 μM (1 h before ionomycin) blocked the effect of ionomycin (Fig. 5G). These results demonstrate a Ca^{2+}-sensitive nature of CaMKIIα-D3R interactions *in vivo*.

To evaluate the role of CaMKIIα-D3R$_{IL3}$ binding *in vivo*, we synthesized a Tat-fusion peptide (Tat-D3Rr). The peptide contains a Tat domain (YGRKKRRQRRR) from the human immunodeficiency virus-type 1 (HIV-1) and a CaMKIIα-binding motif (RILTRQNSQCISIRP) from D3R$_{IL3}$ (Fig. 5H). The arginine-enriched Tat domain renders cell permeability (Aarts et al., 2002;Mao et al., 2005;Liu et al., 2006) and the CaMKIIα-binding motif competes with D3Rs for CaMKII binding in living neurons. In pull-down assays with biotinylated Tat-fusion peptides, Tat-D3Rr but not Tat-D3Rt (a sequence-scrambled control) pulled down recombinant and endogenous CaMKIIα (Fig. S6A), indicating the ability of Tat-D3Rr to bind to CaMKIIα. Tat-D3Rr (5-10μM, 1 h before ionomycin) substantially reduced the ionomycin-stimulated association of the two proteins in striatal/NAc slices, while Tat-D3Rt did not (Fig. 5H). Thus,active CaMKIIα was directly recruited to D3R$_{IL3}$ in response to Ca^{2+} rises. Ionomycin was found to increase serine phosphorylation of D3Rs as detected by an antibody selective for phosphoserine (Fig. 5I). This increase no longer occurred in slices pretreated with Tat-D3Rr (Fig. 5I) or KN93 (Fig. S6B), indicating that the interaction of active CaMKIIα with D3R$_{IL3}$ is required for the ionomycin-stimulated phosphorylation of the receptor. The selectivity of Tat-D3Rr in disrupting the CaMKIIα-D3R interaction was confirmed by the lack of its effect in interfering with the ionomycin-stimulated CaMKIIα interaction with a number of other CaMKII substrates, including NR2B, the cyclin-dependent kinase 5 activator p35, or α-actinin-1 (Fig. S7).

To identify the receptors that might provide a Ca^{2+} entry to trigger the CaMKIIα association to D3Rs, we tested the effect of glutamate receptor activation on the interaction in NAc slices. Glutamate mimicked the effect of ionomycin in stimulating the CaMKIIα-D3R association (Fig. 6A). The effect of glutamate was blocked by KN93 and the NMDA receptor antagonist MK801, but not by KN92 and the AMPA receptor antagonist GYKI52466 (Fig. 6B). Thus, glutamate, through activating NMDA receptors, elevates the CaMKIIα-D3R association. In support of this, NMDA itself induced a concentration-dependent and rapid increase in the association of the two proteins (Fig. 6C and 6D). FPL64176, an activator of L-type voltage-operated Ca^{2+} channels (VOCCs), slightly enhanced the CaMKIIα-D3R interaction, which was blocked by the antagonist nifedipine (Fig. 6E). Together, VOCCs and especially NMDA receptors can provide a Ca^{2+} entry to trigger the CaMKIIα-D3R association.

Activation of phosphatidylinositol (PI)-linked D1Rs (Gαq-coupled) rather than classical cAMP-linked D1Rs (Gαs-coupled) elicits the Ca^{2+} release from intracellular stores through a phospholipase Cβ (PLCβ)-dependent and adenylyl cyclase-independent mechanism (Felder et al., 1989; Undie and Friedman, 1990). To determine if the Ca^{2+} release induced by activating PI-linked D1Rs affects the CaMKIIα-D3R interaction, we examined the effect of activating these receptors on the interaction of the two proteins in NAc slices. Pharmacological activation of PI-linked D1Rs with a selective agonist SKF83959 (Jin et al., 2003) increased the interaction of CaMKIIα with D3Rs (Fig. 6F). This increase was blocked by the D1R antagonist SCH23390, the amino steroid PLCβ inhibitor U73122 (but not its inactive analog U73343), and Tat-CaMKIINtide (Fig. 6F). Thus, the Ca^{2+} release by PI-linked D1Rs possesses the ability to upregulate the CaMKIIα-D3R interaction. The previous data showing the selective activation of CaMKII by PI- but not cAMP-linked D1Rs (Zhen et al., 2004) support this notion.

CaMKIIα-D3R$_{IL3}$ interactions downregulate D3R function

Activation of D3Rs inhibits the adenylyl cyclase-mediated cAMP formation (Ahlgren-Beckendorf and Levant, 2004; Jeanneteau et al., 2006). We next investigated whether the binding of CaMKII to D3R$_{IL3}$ alters the D3R function in inhibiting cAMP formation. In rat accumbal slices, the adenylyl cyclase activator forskolin (1 μM, 20 min) markedly elevated cAMP levels above a baseline of 4.1 ± 0.3 pmol/ml. A D3R selective agonist PD128907 at low concentrations (1–3 nM) significantly reduced the forskolin-activated cAMP accumulation

(Fig. 7A). The selectivity of PD128907 was demonstrated by the observation that the agonist when applied at these sufficiently low concentrations did not alter the forskolin effect in slices from D3R mutant mice (Fig. S8). Co-treatment with ionomycin (10 μM) antagonized the effect of PD128907 (Fig. 7A). The effect of ionomycin was sensitive to KN93 and Tat-CaMKIINtide but not KN92 (Fig. 7A). Furthermore, Tat-D3Rr (8μM, 1 h prior to ionomycin/PD128907) attenuated the effect of ionomycin while Tat-D3Rt did not (Fig. 7B). Neither Tat-D3Rr nor Tat-D3Rt had any effect on the forskolin-stimulated cAMP formation or on the inhibition of forskolin-stimulated cAMP formation by PD128907 (data not shown). These data indicate that Ca^{2+}-activated CaMKII associates with D3Rs and reduces D3R efficacy in inhibiting cAMP production.

More experiments were performed in accumbal slices to evaluate the role of CaMKII in regulating dopamine-mediated cAMP signaling. We found that dopamine (5 μM) consistently elevated cAMP levels. This elevation was reduced by Tat-D3Rr (Fig. 7C). Thus, CaMKII-D3R interactions inhibit the cAMP response to dopamine. Tat-D3Rr alone did not alter basal cAMP levels (Fig. 7C), suggesting a minimal impact of CaMKIIα-$D3R_{IL3}$ interactions to D3R function under basal conditions, in which relatively lower levels of basal CaMKIIα-$D3R_{IL3}$ binding would be anticipated. It is noteworthy that the dopamine concentration (5 μM) applied here is within the physiological range of evoked dopamine release in striatal slice preparations (Jones et al., 1998). In separate experiments, the D1R antagonist SCH23390 blocked the dopamine-stimulated cAMP response (Fig. 7D), indicating that D1R activation largely mediates the positive cAMP response to dopamine. In contrast to the D1R antagonist, the highly selective D3R antagonist NGB2904, when incubated at 50 nM (EC_{50} of 14.4 nM and 1280.0 nM for D3 and D2 receptors, respectively; Yuan et al., 1998;Grundt et al., 2005), slightly increased the cAMP response to dopamine (although $P > 0.05$, Fig. 7D). NGB2904 alone increased basal cAMP concentrations, indicating a tonic D3R activity in inhibiting basal cAMP formation.

CaMKII-D3R interactions further impact downstream effectors of cAMP/protein kinase A (PKA). In accumbal slices, as shown in Fig. 7E, Tat-D3Rr markedly reduced the dopamine-stimulated phosphorylation of cAMP-responsive element binding protein (CREB), a nuclear transcription factor downstream to PKA activation. Tat-D3Rs also reduced the dopamine-stimulated expression of c-Fos, an immediate early gene downstream to CREB (Fig. 7F). In addition to CREB and c-Fos, we examined another target of PKA at excitatory synapses. PKA phosphorylated AMPA receptor GluR1 subunits at serine 845 in mouse striatal slices treated with the D1R agonist SKF81297 (Snyder et al., 2000). Similarly, we observed that SKF81297 increased protein levels of phospho-GluR1 at serine 845 (pGluR1-S845) in synaptosomal fractions from rat accumbal slices (Fig. 7G). A higher level of pGluR1-S845 was also seen in the PSD fraction (Fig. 7G), confirming that the event occurred at synaptic sites. Tat-D3Rr was able to reduce the SKF81297-stimulated GluR1 phosphorylation in synaptosomes (Fig. 7H), indicating that D3Rs are restored to inhibit the PKA-mediated GluR1 phosphorylation. Together, our observations demonstrate that CaMKII inhibits D3R function. As illustrated in Fig. 7I, under basal conditions, CaMKII interacts with D3Rs at a low level. D3Rs, due to their higher affinity for dopamine than D1/D2 receptors (Sokoloff et al., 1992), are activated by basal levels of dopamine to inhibit adenylyl cyclase. When dopamine release is enhanced, the inhibitory tone of D3Rs is suppressed by the Ca^{2+}-induced interaction of CaMKII with $D3R_{IL3}$, which, in concert with D1R stimulation, augments the cAMP/PKA response to dopamine.

A further attempt was made to explore a possible role of our CaMKIIα-D3R interaction model in modulating another key downstream effector of D3Rs. D3Rs expressed in heterologous cells activate extracellular signal-regulated protein kinases 1 and 2 (ERK1/2 or p44/p42) via the Gβγ pathway (Cussac et al., 1999; Beom et al., 2004). In HEK293 cells transiently transfected

with D3Rs, we found a similar transient increase in ERK1/2 phosphorylation following dopamine application (Fig. S9A). This was blocked by NGB2904, confirming the role of D3Rs in mediating this event (Fig. S9B). Noticeably, in HEK293 cells co-transfected with D3Rs and CaMKIIα, ionomycin (2 μM) reduced the dopamine-stimulated ERK2 phosphorylation (Fig. S9C). Tat-D3Rr but not Tat-D3Rt reversed the effect of ionomycin (Fig. S9C). In accumbal slices, activation of D3Rs with PD128907 increased ERK2 phosphorylation, which was reduced by ionomycin (Fig. S9D). Tat-D3Rr antagonized the effect of ionomycin, while Tat-D3Rt did not (Fig. S9D). These data indicate that the interaction of CaMKIIα with D3Rs suppresses the ability of D3Rs to phosphorylate ERK1/2 in heterologous cells and neurons.

CaMKIIα-D3R$_{IL3}$ interactions suppress the D3R-mediated inhibition of motor activity

We extended our molecular observations to behavioral experiments to investigate whether regulated CaMKIIα-D3R$_{IL3}$ interactions modulate behavioral responsiveness to dopamine stimulation. Cocaine is known to stimulate motor activity through a mechanism that results in elevated synaptic dopamine levels. Given that postsynaptic D3Rs are generally inhibitory to stimulant-induced motor activity (Xu et al., 1997; Bahi et al., 2005; Richtand, 2006; Pritchard et al., 2007), we speculated that cocaine would suppress D3Rs by enhancing the interaction of CaMKIIα with D3Rs, which participates in the regulation of the motor response to cocaine. Consistent with this model, cocaine at 20 mg/kg markedly increased the formation of CaMKIIα-D3R$_{IL3}$ complexes in the rat NAc (Fig. 8A). A slight increase in this complex formation was induced by cocaine at 5 mg/kg (19.3 ± 0.03% over control). The effect of cocaine (20 mg/kg) was blocked by pretreatment with an intravenous (i.v.) injection of the interfering peptide Tat-D3Rr (3 nmol/g, 1.5 h before cocaine). The control peptide (Tat-D3Rt) had no effect. Using fluorescently tagged peptides (FITC-Tat-D3Rr), the dynamic presence of these systemically active and cell-permeable peptides in striatal tissues was demonstrated after a single injection (Fig. 8B). Intracellular uptake of a FITC-Tat-D3Rr peptide, but not a control peptide containing HIV-1 Tat residues 38 to 48 (KALGISYGRKK; Tat38-48) that lie outside the transduction domain, was evident in accumbal neurons following an i.v. injection (Fig. 8C). Interestingly, in open field locomotor activity assays, Tat-D3Rr but not Tat-D3Rt reduced the horizontal activity induced by cocaine (20 mg/kg) while neither peptide had any effect on spontaneous locomotion (Fig. 8D-F). To determine whether the effect of systemic peptides primarily occurs in the local NAc, a microinjection study targeting the NAc was performed in freely moving rats. A local injection of Tat-D3Rr (15 pmol, 1 h prior to cocaine) produced the same effect as that observed following a systemic injection (Fig. 8G and H). Additionally, an intra-accumbal injection of KN93 but not KN92 (10 nmol) reduced the effect of cocaine on the formation of CaMKIIα-D3R complexes (data not shown). In WT mice, Tat-D3Rr reduced the cocaine-stimulated locomotion whereas no such effect was observed in D3R mutant mice (Fig. 8I). Together, these results support a model in which cocaine recruits CaMKIIα to D3Rs to downregulate the D3R function in inhibiting motor responses to cocaine, which ultimately enhances behavioral sensitivity to cocaine stimulation.

Discussion

A new discovery in this study is the protein-protein interaction between CaMKIIα and D3Rs in accumbal neurons. The interaction is region-selective since it did not occur in other brain areas, including the substantia nigra and the ventral tegmental area. The interaction involves the consensus CaMKII-binding sequence (I/L)*X*R*XX*(S/T) (White et al., 1998) located in the third intracellular loop of D3Rs. Another important characteristic of the CaMKIIα-D3R interaction is its Ca^{2+} sensitivity. Activation of CaMKIIα by Ca^{2+}/CaM enhanced the binding affinity of the kinase for D3Rs *in vitro*. In accumbal neurons *in vivo*, activation of NMDA receptors, VOCCs, and PI-linked D1Rs that elicit the Ca^{2+} release from intracellular stores increased the CaMKIIα-D3R interaction, providing the linkage of these Ca^{2+} routes to D3R

physiology. Moreover, autophosphorylation of CaMKIIα regulates the CaMKIIα-D3R interaction. This was shown by the findings that the autophosphorylation at T286 further enhanced the affinity of the kinase for D3Rs and sustained the kinase association with D3Rs after Ca^{2+} was chelated with EGTA. Thus, the autophosphorylated CaMKIIα is believed to still have an influence on D3R function even after a transient Ca^{2+} rise recovers to the original level.

The NMDA receptor was the first receptor that was identified to be bound by CaMKIIα at synaptic sites (Gardoni et al., 1998; Leonard et al, 1999). In response to Ca^{2+} influx, CaMKIIα is recruited to the PSD of excitatory synapses by its increased association with the NMDA receptor NR2B subunit (Colbrain, 2004; Bayer et al., 2006). The Ca^{2+}-evoked CaMKIIα-D3R interaction identified in the current work suggests a new recruiter of CaMKII to the PSD. This is supported by the distribution of abundant D3Rs in the purified PSD (this study). The fact that multiple synaptic receptors interact with CaMKII and recruit it to presumably distinct submembranous microdomains is in good accordance with the multivalent and multifunctional nature of holoenzymes and with the high abundance of the enzyme at synaptic sites.

The $D3R_{IL3}$ is a critical region for Gαi/o-coupling (Ilani et al., 2002), and activation of D3Rs inhibits adenylyl cyclase in heterologous cells (Ahlgren-Beck and Levant, 2004; Sokoloff et al., 2006). In accumbal neurons, the D3R-mediated inhibition of forskolin-stimulated cAMP accumulation was established in this study. Notably, the D3R efficacy was subject to the regulation by Ca^{2+} because the cytoplasmic Ca^{2+} rise induced by an ionophore reversed the effect of a D3R agonist. This Ca^{2+} regulation relies on the CaMKII activation and the subsequent association of activated CaMKII with D3Rs as demonstrated by the findings that both the CaMKII activation inhibitors (KN93 and CaMKIINtide) and Tat-D3Rr, which disrupted the CaMKIIα-$D3R_{IL3}$ binding, antagonized the effect of the Ca^{2+} ionophore. Together, the Ca^{2+}-triggered recruitment of CaMKII to D3Rs suppresses the D3R efficacy and thus relieves the inhibitory tone of D3Rs on the adenylyl cyclase/cAMP cascade. In this model, a state-dependent nature of CaMKII regulation is recognized (see Fig. 7I). Under basal conditions, the regulation is less significant due to a lower level of CaMKII binding to D3Rs. As a result, D3Rs become tonically active in inhibiting cAMP production. Of note, the D3R is the only subtype with an affinity (*K*i = 30 nM; Sokoloff et al., 1992) within the nanomolar range of basal dopamine concentrations at synapses (~ 50 nM; Ross, 1991). This allows D3Rs to respond to baseline dopamine. When transformed to a stimulated state in which the synaptic dopamine level is increased to the micromolar range, CaMKII is recruited to D3Rs by Ca^{2+} to depress the D3R efficacy. This, in concert with the simultaneously activated D1 efficacy (Surmeier et al., 1996; Ridray et al., 1998), would produce a net upregulation of the cAMP-PKA pathway and its downstream targets, including CREB phosphorylation, c-Fos expression, and AMPA receptor phosphorylation (Snyder et al., 2000; Zhang et al., 2004; Jiao et al., 2007). Together, the CaMKII-D3R coupling discovered here suggests a new model of the integration of limbic dopamine signals under basal and stimulated conditions.

D1R activation contributes to cocaine-stimulated motor activity. In response to cocaine, synaptic dopamine levels are increased, which in turn activates D1Rs on striatonigral neurons. Through cAMP/PKA, D1Rs enhance excitability of these neurons to glutamate, thereby increasing outflow of the direct striatonigral pathway and motor activity (Surmeier et al., 2007). In contrast to D1Rs, D3Rs inhibit the cAMP-PKA pathway. Thus, D3Rs are believed to exert an inhibitory effect on dopamine-mediated motor activity. Indeed, D3R mutant mice displayed hyperactivity in a novel environment (Accili et al., 1996; Xu et al., 1997), indicating an inhibitory tone of postsynaptic D3Rs on normal motor activity (Koeltzow et al., 1998). D3Rs also suppress motor responsiveness to cocaine as evidenced by the fact that cocaine at a low dose (5 mg/kg) induced a significantly greater motor response in D3R mutant mice than

in WT mice (Xu et al., 1997). Other behavioral studies utilizing D3R mutant mice or D3R-preferring agents generally support this view (Bahi et al., 2005; Richtand, 2006; Pritchard et al., 2007). However, the D3R-mediated inhibition is subject to downregulation in response to increasing doses of cocaine because cocaine at higher doses (20–40 mg/kg) induced similar increases in motor responses in D3R mutant mice as compared to WT mice (Xu et al., 1997). Indeed, in this study, we observed a suppression of D3R function by cocaine via a mechanism involving CaMKII. This was demonstrated by the findings that 1) cocaine dose-dependently increased the association of CaMKII with D3Rs, and 2) the disruption of this association by Tat-D3Rr restored the ability of D3Rs to suppress the motor response to cocaine (20 mg/kg) in rats and WT mice but not in D3R mutant mice. Tat-D3Rr also restored the efficiency of D3Rs to inhibit the D1R-mediated phosphorylation of synaptic AMPA receptors at a PKA-sensitive site (serine 845) in accumbal neurons. Together, through a specific protein-protein interaction between CaMKII and D3Rs, cocaine transiently releases the D3R-mediated 'brake' on behavioral responses to the stimulant. This dynamic downregulation of D3R function could enhance behavioral sensitivity to cocaine stimulation.

Experimental Procedures

Animals—Adult male Wistar rats weighting 200–225 g (Charles River, New York, NY), adult WT mice, and mutant mice lacking D3Rs were individually housed at 23°C and humidity of 50 ± 10% with food and water available *ad libitum*. The animal room was on a 12/12 h light/dark cycle with lights on at 0700. All animal use procedures were in strict accordance with the NIH *Guide for the Care and Use of Laboratory Animals* and were approved by the Institutional Animal Care and Use Committee.

Protein extraction—Rats were anesthetized with 2.5–3% isoflurane and decapitated. Brains were removed and coronal sections were cut. Bilateral punches of the local NAc (core and shell) or other brain regions were obtained using punch corers. Samples were removed into a microtube containing ice-cold sample buffer (20 mM Tris-HCl, pH 7.4, 1 mM dithiothreitol, 10 mM NaF, 2 mM Na_3VO_4, 1 mM EDTA, 1 mM EGTA, 5 μM microcystin-LR, and 0.5 mM phenylmethylsulfonyl fluoride), and homogenized by sonication. Homogenates were centrifuged at 700 *g* for 10 min at 4°C. The supernatant was centrifuged at 10,000 *g* at 4°C for 30 min to obtain the P2 pellet (synaptosomal fraction). After solubilization (see supplemental experimental procedures), protein concentrations were determined.

Cloning, expression, and purification of GST-fusion proteins—The cDNA fragments encoding the $D3R_{IL2}$(D127-R149), $D3R_{IL3}$(R210-Q375), $D3R_{IL3}$(R210-P239), $D3R_{IL3}$(Q240-Q375), $D3R_{IL3}$(H269-Q375), $D3R_{IL3}$(R345-Q375), $D2R_{IL3}$(I210-V270), $CaMKII\alpha_{CD}$(L91-S272), $CaMKII\alpha_{RD}$(H273-S314), or $CaMKII\alpha_{AD}$(G315-H478) were generated by PCR amplification from full-length cDNA clones. These fragments were subcloned into BamHI-EcoRI sites of the pGEX4T-3 plasmid (Amersham Biosciences, Arlington Heights, IL) or *Spe*I-*Xho*I sites of the pET-41a(+) plasmid (Novagen, Madison, WI). Initiation methionine residues and stop codons were also incorporated where appropriate. To confirm appropriate splice fusion, all constructs were sequenced. GST-fusion proteins were expressed in *E. coli* BL21 cells (Amersham) or BL21(DE3)pLysE cells (Novagen) and purified from bacterial lysates as described by the manufacturer. GST- or His-tagged full-length CaMKIIα (M1-H478) and GST-tagged full-length CaMKIV (M1-Y473) were expressed and purified via a baculovirus/Sf9 insect cell expression system.

Affinity purification (pull-down) assay—Solubilized accumbal extracts (50–100 μg of protein) were diluted with 1X PBS/1% Triton X-100 and incubated with 50% (v/v) slurry of glutathione-Sepharose 4B beads (Amersham) saturated with GST alone or with the indicated GST-fusion protein (5–10μg) for 2–3 h at 4°C. Beads were washed four times with 1X PBS/

1% Triton X-100. Bound proteins were eluted with 2X lithium dodecyl sulfate (LDS) sample buffer, resolved by SDS-PAGE, and immunoblotted with a specific antibody.

In vitro binding assay—GST-fusion proteins (1–5 μg) in PBS were digested with 0.2 NIH unit of thrombin (Sigma, St. Louis, MO) for 2 h at room temperature. The reaction was stopped by adding PMSF (10 μM). GST was removed by glutathione Sepharose (Amersham). The supernatant was equilibrated to binding buffer (200 mM NaCl, 0.2% Triton X-100, 0.1 mg/ml BSA, and 50 mM Tris, pH, 7.5) with or without 0.5 mM $CaCl_2$, 1 μM CaM, 1 mM EGTA, or 50 μM ATP as indicated. In some experiments, His-tagged CaMKIIα WT (~57 kDa), WT pCaMKIIα, CaMKIIα mutants (~50 kDa), or CaM were used. Binding reactions were initiated by adding purified GST-fusion proteins and were remained at 4°C for 2–3 h unless otherwise indicated. GST-fusion proteins were precipitated using 100 μl of 10% glutathione Sepharose. The precipitate was washed three times with binding buffer. Bound proteins were eluted with 2X LDS loading buffer, resolved by SDS-PAGE, and immunoblotted with a specific antibody.

cAMP enzyme immunoassay—After incubation with drugs indicated for 20–30 min at room temperature, accumbal slices were homogenized in 0.1 M HCl solution for 15 min with gentle shaking and spun in the microcentrifuge tubes. cAMP concentration of the supernatant was measured using the Direct cAMP Enzyme Immunoassay (EIA) Kit (Assay Designs, Ann Arbor, MI) following the manufacturer's instruction. Protein concentrations were determined using a BCA Protein Assay kit (Pierce).

Behavioral assessments—Locomotion in an open field was evaluated as described previously (Liu et al., 2006).

Supplementary Material

Refer to Web version on PubMed Central for supplementary material.

Acknowledgements

This work was supported by NIH grants DA10355 (J.Q.W.), MH61469 (J.Q.W.), DA14644 (M.X.), and DA17323 (M.X.), and by a grant from Saint Luke's Hospital Foundation. We thank Dr. Howard Schulman and Dr. K. Ulrich Bayer for providing T286A, T286D, and T305/306 mutant vectors, Dr. Xiaoming Xia for help in preparing plasmids, Dr. Kim A. Neve for critical reading of the manuscript, Ms. Lucy S. Wang, Dr. Xiaoqiang Yu, and Dr. Nilofer Qureshi for technical support and comments, and Dr. Amy Hauck Newman (Medicinal Chemistry Section, NIDA-IRP) and Dr. Zheng-Xiong Xi (NIDA-IRP) for providing NGB2904.

References

Aarts M, Liu Y, Liu L, Besshoh S, Arundine M, Gurd JW, Wang YT, Salter MW, Tymianski M. Treatment of ischemic brain damage by perturbing NMDA receptor-PSD-95 protein interactions. Science 2002;298:846–850. [PubMed: 12399596]

Accili D, Fishburn CS, Drago J, Steiner H, Lachowicz JE, Park BH, Gauda EB, Lee EJ, Cool MH, Sibley DR, Gerfen CR, Westphal H, Fuchs S. A targeted mutation of the D_3 dopamine receptor gene is associated with hyperactivity in mice. Proc Natl Acad Sci USA 1996;93:1945–1949. [PubMed: 8700864]

Ahlgren-Beckendorf JA, Levant B. Signaling mechanisms of the D3 dopamine receptor. J Recept Signal Transduct Res 2004;24:117–130. [PubMed: 15521358]

Bahi A, Boyer F, Bussard G, Dreyer JL. Silencing dopamine D3-receptors in the nucleus accumbens shell *in vivo* induces changes in cocaine-induced hyperlocomotion. Eur J Neurosci 2005;21:3415–3426. [PubMed: 16026479]

Bayer KU, Koninck PD, Leonard AS, Hell JW, Schulman H. Interaction with the NMDA receptor locks CaMKII in an active conformation. Nature 2001;411:801–805. [PubMed: 11459059]

Bayer KU, LeBel E, McDonald GL, O'Leary H, Schulman H, Koninck PD. Transition from reversible to persistent binding of CaMKII to postsynaptic sites and NR2B. J Neurosci 2006;26:1164–1174. [PubMed: 16436603]

Beom SR, Cheong D, Torres G, Caron MG, Kim KM. Comparative studies of molecular mechanisms of dopamine D_2 and D_3 receptors for the activation of extracellular signal-regulated kinase. J Biol Chem 2004;279:28304–28314. [PubMed: 15102843]

Bouthenet ML, Souil E, Martres MP, Sokoloff P, Giros B, Schwartz JC. Localization of dopamine D3 receptor mRNA in the rat brain using *in situ* hybridization histochemistry: comparison with dopamine D2 receptor mRNA. Brain Res 1991;564:203–219. [PubMed: 1839781]

Chang BH, Mukherji S, Soderling TR. Characterization of a calmodulin kinase II inhibitor protein in brain. Proc Natl Acad Sci USA 1998;95:10890–10895. [PubMed: 9724800]

Colbran RJ. Targeting of calcium/calmodulin-dependent protein kinase II. Biochem J 2004;378:1–16. [PubMed: 14653781]

Colbran RJ, Brown AM. Calcium/calmodulin-dependent protein kinase II and synaptic plasticity. Curr Opin Neurobiol 2004;14:318–327. [PubMed: 15194112]

Colbran RJ, Soderling TR. Calcium/calmodulin-independent autophosphorylation sites of calcium/calmodulin-dependent protein kinase II. Studies on the effect of phosphorylation of threonine 305/306 and serine 314 on calmodulin binding using synthetic peptides. J Biol Chem 1990;265:11213–11219. [PubMed: 2162839]

Cussac D, Newman-Tancredi A, Pasteau V, Millan MJ. Human dopamine D3 receptors mediate mitogen-activated protein kinase activation via a phosphatidylinositol 3-kinase and an atypical protein kinase C-dependent mechanism. Mol Pharmacol 1999;56:1025–1030. [PubMed: 10531409]

Felder CC, Jose PA, Axelrod J. The dopamine-1 agonist, SKF82526, stimulates phospholipase-C activity independent of adenylate cyclase. J Pharmacol Exp Ther 1989;248:171–175. [PubMed: 2563286]

Gardoni F, Caputi A, Cimino M, Pastorino L, Cattabeni F, Di Luca M. Calcium/calmodulin-dependent protein kinase II is associated with NR2A/B subunits of NMDA receptor in postsynaptic densities. J Neurochem 1998;71:1733–1741. [PubMed: 9751209]

Griffith LC. Regulation of calcium/calmodulin-dependent protein kinase II activation by intramolecular and intermolecular interactions. J Neurosci 2004;24:8394–8398. [PubMed: 15456810]

Grundt P, Carlson EE, Cao J, Bennett CJ, McElveen E, Taylor M, Luedtke RR, Newman AH. Novel heterocyclic trans olefin analogues of N{4-[4-(2,3-dichlorophenyl)piperazin-1-yl]butyl} arylcarboxamides as selective probes with high affinity for the dopamine D3 receptor. J Med Chem 2005;48:839–848. [PubMed: 15689168]

Hashimoto Y, Soderling TR. Calcium · calmodulin-dependent protein kinase II and calcium · phospholipid-dependent protein kinase activities in rat tissues assayed with a synthetic peptide. Arch Biochem Biophy 1987;252:418–425.

Heidbreder CA, Gardner EL, Xi ZX, Thanos PK, Mugnaini M, Hagan JJ, Ashby CR Jr. The role of central dopamine D3 receptors in drug addiction: a review of pharmacological evidence. Brain Res Rev 2005;49:77–105. [PubMed: 15960988]

Hudman A, Schulman H. Neuronal Ca^{2+}/calmodulin-dependent protein kinase II: the role of structure and autoregulation in cellular function. Annu Rev Biochem 2002;71:473–510. [PubMed: 12045104]

Ilani T, Fishburn CS, Levavi-Sivan B, Carmon S, Raveh L, Fuchs S. Coupling of dopamine receptors to G proteins: studies with chimeric D2/D3 dopamine receptors. Cell Mol Neurobiol 2002;22:47–56. [PubMed: 12064517]

Jeanneteau F, Funalot B, Jankovic J, Deng H, Lagarde JP, Lucotte G, Sokoloff P. A functional variant of the dopamine D3 receptor is associated with risk and age-at-onset of essential tremor. Proc Natl Acad Sci USA 2006;103:10753–10758. [PubMed: 16809426]

Jiao H, Zhang L, Gao F, Lou D, Zhang J, Xu M. Dopamine D1 and D3 receptors oppositely regulate NMDA- and cocaine-induced MARK signaling via NMDA receptor phosphorylation. J Neurochem 2007;103:840–848. [PubMed: 17897358]

Jin LQ, Goswami S, Cai G, Zhen X, Friedman E. SKF83959 selectively regulates phosphatidylinositol-linked D_1 dopamine receptors in rat brain. J Neurochem 2003;85:378–386. [PubMed: 12675914]

Jones SR, Gainetdinov RR, Wightman RM, Caron MG. Mechanisms of amphetamine action revealed in mice lacking the dopamine transporter. J Neurosci 1998;18:1979–1986. [PubMed: 9482784]

Kelly PT, McGuinness TL, Greengard P. Evidence that the major postsynaptic density protein is a component of a Ca^{2+}/calmodulin-dependent protein kinase. Proc Natl Acad Sci USA 1984;81:945–949. [PubMed: 6583689]

Koeltzow TE, Xu M, Cooper DC, Hu XT, Tonegawa S, Wolf ME, White FJ. Alterations in dopamine release but not dopamine autoreceptor function in dopamine D3 receptor mutant mice. J Neurosci 1998;18:2231–2238. [PubMed: 9482807]

Leonard AS, Lim IA, Hemsworth DE, Horne MC, Hell JW. Calcium/calmodulin-dependent protein kinase II is associated with the *N*-methyl-D-aspartate receptor. Proc Natl Acad Sci USA 1999;96:3239–3244. [PubMed: 10077668]

Lisman J, Schlman H, Cline H. The molecular basis of CaMKII function in synaptic and behavioral memory. Nat Rev Neurosci 2002;3:175–190. [PubMed: 11994750]

Liu XY, Chu XP, Mao LM, Wang M, Lan HX, Li MH, Zhang GC, Parelkar NK, Fibuch EE, Haines M, Neve KA, Liu F, Xiong ZG, Wang JQ. Modulation of D2R-NR2B interactions in response to cocaine. Neuron 2006;52:897–909. [PubMed: 17145509]

Mao L, Yang L, Tang Q, Samdani S, Zhang G, Wang JQ. The scaffold protein Homer1b/c links metabotropic glutamate receptor 5 to extracellular signal-regulated protein kinase cascades in neurons. J Neurosci 2005;25:2741–2742. [PubMed: 15758184]

Meyer T, Hanson PI, Stryer L, Schulman H. Calmodulin trapping by calcium-calmodulin-dependent protein kinase. Science 1992;256:1199–1201. [PubMed: 1317063]

Neve KA, Seamans JK, Trantham-Davidson H. Dopamine receptor signaling. J Recept Signal Transduct Res 2004;24:165–205. [PubMed: 15521361]

Omkumar RV, Kiely MJ, Rosenstein AJ, Min KT, Kennedy MB. Identification of a phosphorylation site for calcium/calmodulin-dependent protein kinase II in the NR2B subunit of the *N*-methyl-D-aspartate receptor. J Biol Chem 1996;271:31670–31678. [PubMed: 8940188]

Pritchard LM, Newman AH, McNamara RK, Logue AD, Taylor B, Welge JA, Xu M, Zhang J, Richtand NM. The dopamine D3 receptor antagonist NGB 2904 increases spontaneous and amphetamine-stimulated locomotion. Pharmacol Biochem Behav 2007;86:718–726. [PubMed: 17408730]

Richtand NM. Behavioral sensitization, alternative splicing, and D3 dopamine receptor-mediated inhibitory function. Neuropsychopharmacology 2006;31:2368–2375. [PubMed: 16855531]

Ridray S, Griffon N, Mignon V, Souil E, Carboni S, Diaz J, Schwartz JC, Sokoloff P. Coexpression of dopamine D1 and D3 receptors in islands of Calleja and shell of nucleus accumbens of the rat: opposite and synergistic functional interactions. Eur J Neurosci 1998;10:1676–1686. [PubMed: 9751140]

Ross SB. Synaptic concentration of dopamine in the mouse striatum in relationship to the kinetic properties of the dopamine receptors and uptake mechanism. J Neurochem 1991;56:22–29. [PubMed: 1824780]

Snyder GL, Allen PB, Fienberg AA, Valle CG, Huganir RL, Nairn AC, Greengard P. Regulation of phosphorylation of the GluR1 AMPA receptor in the neostriatum by dopamine and psychostimulants *in vivo*. J Neurosci 2000;20:4480–4488. [PubMed: 10844017]

Sokoloff P, Giros B, Martres MP, Bouthenet ML, Schwartz JC. Molecular cloning and characterization of a novel dopamine receptor (D3) as a target for neuroleptics. Nature 1990;347:146–151. [PubMed: 1975644]

Sokoloff P, Diaz J, Le Foll B, Guillin O, Leriche L, Bezard E, Gross C. The dopamine D3 receptor: a therapeutic target for the treatment of neuorpsychiatric disorders. CNS Neurol Disord Drug Targets 2006;5:25–43. [PubMed: 16613552]

Sokoloff P, Martres MP, Giros B, Bouthenet ML, Schwartz JC. The third dopamine receptor (D3) as a novel target for antipsychotics. Biochem Pharmacol 1992;43:659–666. [PubMed: 1347215]

Strack S, Choe S, Lovinger DM, Colbran RJ. Translocation of autophosphorylated calcium/calmodulin-dependent protein kinase II to the postsynaptic density. J Biol Chem 1997;272:13467–13470. [PubMed: 9153188]

Strack S, McNeill RB, Colbran RJ. Mechanism and regulation of calcium/calmodulin-dependent protein kinase II targeting to the NR2B subunit of the *N*-methyl-D-aspartate receptor. J Biol Chem 2000;275:23798–23806. [PubMed: 10764765]

Surmeier DJ, Ding J, Day M, Wang Z, Shen W. D1 and D2 dopamine-receptor modulation of striatal glutamatergic signaling in striatal medium spiny neurons. TINS 2007;30:228–235. [PubMed: 17408758]

Surmeier DJ, Song WJ, Yan Z. Coordinated expression of dopamine receptors in neostriatal medium spiny neurons. J Neurosci 1996;16:6579–6591. [PubMed: 8815934]

Undie AS, Friedman E. Stimulation of a dopamine D_1 receptor enhances inositol phosphates formation in rat brain. J Pharmacol Exp Ther 1990;253:987–992. [PubMed: 1972756]

Vest RS, Davies KD, O'Leary H, Prot JD, Bayer KU. Dual mechanism of a natural CaMKII inhibitor. Mol Biol Cell 2007;18:5024–5033. [PubMed: 17942605]

White RR, Kwon YG, Taing M, Lawrence DS, Edelman AM. Definition of optimal substrate recognition motifs of Ca^{2+}-calmodulin-dependent protein kinases IV and II reveals shared and distinctive features. J Biol Chem 1998;273:3166–3179. [PubMed: 9452427]

Xu M, Koeltzow TE, Santiago GT, Moratalla R, Cooper DC, Hu XT, White NM, Graybiel AM, White FJ, Tonegawa S. Dopamine D3 receptor mutant mice exhibit increased behavioral sensitivity to concurrent stimulation of D1 and D2 receptors. Neuron 1997;19:837–848. [PubMed: 9354330]

Yang E, Schulman H. Structural examination of autoregulation of multifunctional calcium/calmodulin-dependent protein kinase II. J Biol Chem 1999;274:26199–26208. [PubMed: 10473573]

Yuan J, Chen X, Brodbeck R, Primus R, Braun J, Wasley JW, Thurkauf A. NGB 2904 and NGB 2849: two highly selective dopamine D3 receptor antagonists. Bioorg Med Chem Lett 1998;8:2715–2718. [PubMed: 9873609]

Zhang L, Lou D, Jiao H, Zhang D, Wang X, Xia Y, Zhang J, Xu M. Cocaine-induced intracellular signaling and gene expression are oppositely regulated by the dopamine D1 and D3 receptors. J Neurosci 2004;24:3344–3354. [PubMed: 15056714]

Zhen X, Goswami S, Abdali SA, Gil M, Bakshi K, Friedman E. Regulation of cyclin-dependent kinase 5 and calcium/calmodulin-dependent protein kinase II by phosphatidylinositol-linked dopamine receptor in rat brain. Mol Pharmacol 2004;66:1500–1507. [PubMed: 15286209]

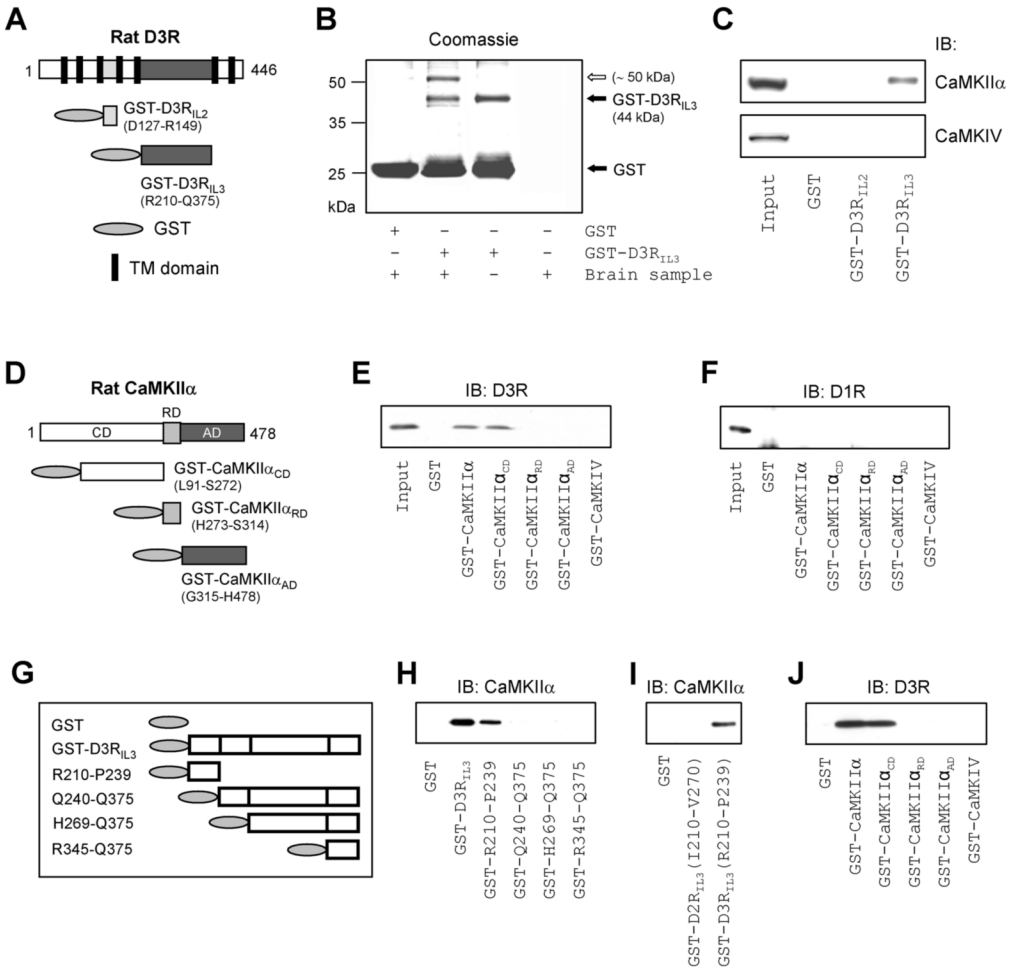

Figure 1. Association of CaMKIIα with D3Rs

(A) GST-fusion proteins derived from rat D3Rs with 7 transmembrane (TM) domains. **(B)** Coomassie staining of a gel resolved from pull-down assays with rat accumbal lysates. An open arrow indicates a protein (~50 kDa) pulled down by GST-D3R$_{IL3}$. **(C)** GST-D3R$_{IL3}$ precipitated CaMKIIα from rat accumbal lysates. **(D)** GST-fusion proteins derived from rat CaMKIIα. **(E and F)** GST-CaMKIIα and GST-CaMKIIα$_{CD}$ precipitated D3Rs (E), but not D1Rs (F), from rat accumbal lysates. **(G)** GST-fusion proteins derived from D3R$_{IL3}$. **(H–J)** Results from *in vitro* binding assays with GST-fusion proteins and purified CaMKIIα (H and I) or D3R$_{IL3}$ (J). Precipitated proteins from pull-down assays (C, E, and F) and proteins bound to CaMKIIα or D3R$_{IL3}$ from *in vitro* binding assays (H–J) were visualized with immunoblots (IB) using the specific antibodies as indicated.

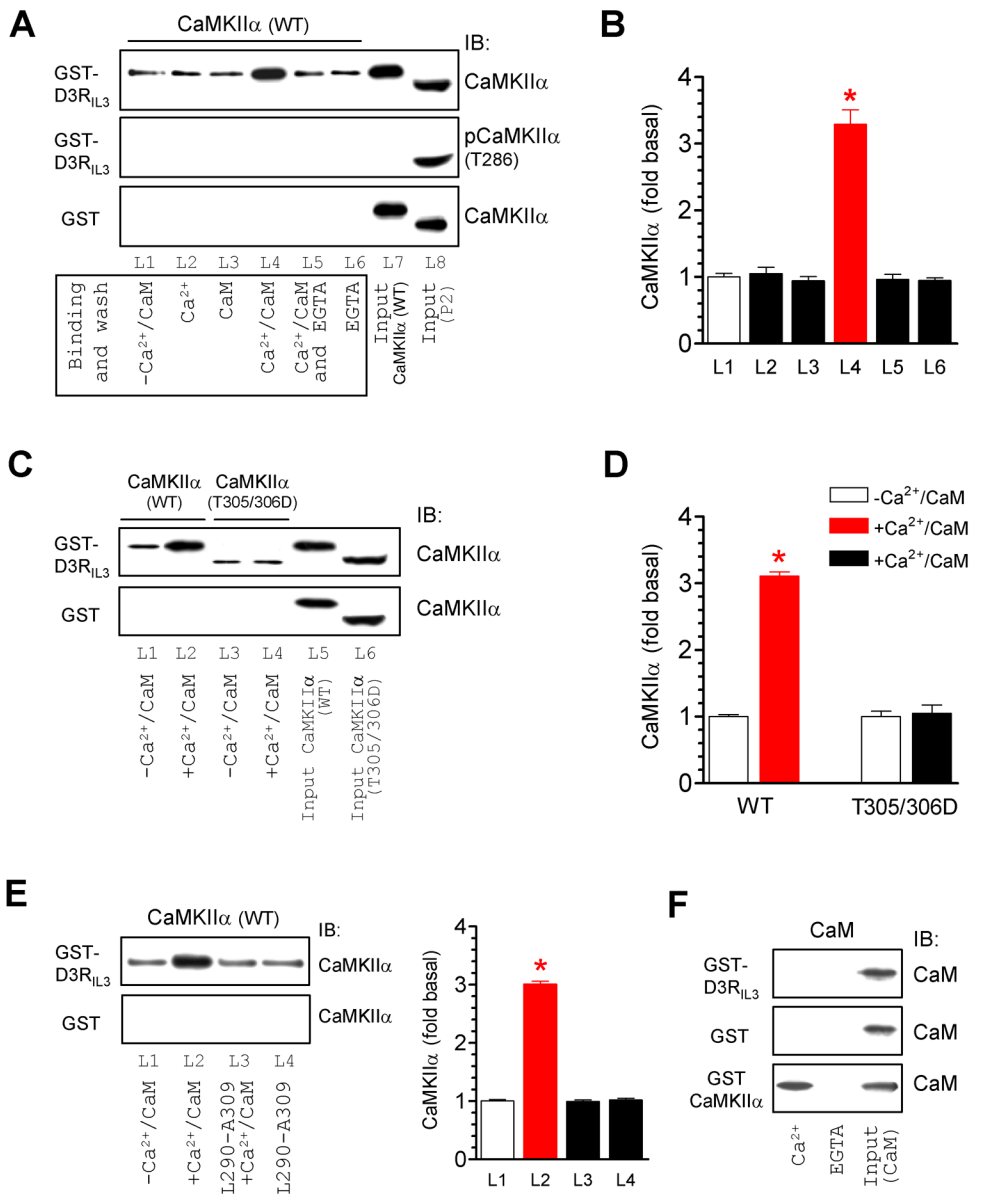

Figure 2. Ca^{2+}/CaM-regulated CaMKIIα binding to D3R$_{IL3}$

(A and B) Addition of Ca^{2+}/CaM increased the CaMKIIα binding to GST-D3R$_{IL3}$. Note that, in the middle panel of Fig. 2A, CaMKIIα was not autophosphorylated at T286 in binding assays lacking ATP (L1-L6) as opposed to T286-autophosphorylated CaMKIIα detected in the synaptosomal fraction (P2) from the rat NAc (L8) with a phospho-specific antibody. **(C and D)** Addition of Ca^{2+}/CaM did not alter the binding of CaMKIIα T305/306D mutant to GST-D3R$_{IL3}$. **(E)** Co-addition of an inhibitory peptide (L290-A309) prevented an increase in the CaMKIIα-D3R$_{IL3}$ binding induced by Ca^{2+}/CaM. **(F)** CaM did not bind to GST-D3R$_{IL3}$ or GST whereas it bound to GST-CaMKIIα in a Ca^{2+}-dependent manner. Binding assays were performed between His-tagged WT CaMKIIα (~57 kDa), T305/306D mutant (~50 kDa), or CaM proteins and immobilized GST, GST-D3R$_{IL3}$, or GST-CaMKIIα in the presence or absence of $CaCl_2$ (0.5 mM), CaM (1 μM), EGTA (1 mM), or L290-A309 (5 μM). Data are presented as means ± SEM for 3–6 experiments per group. *$p < 0.05$ versus L1.

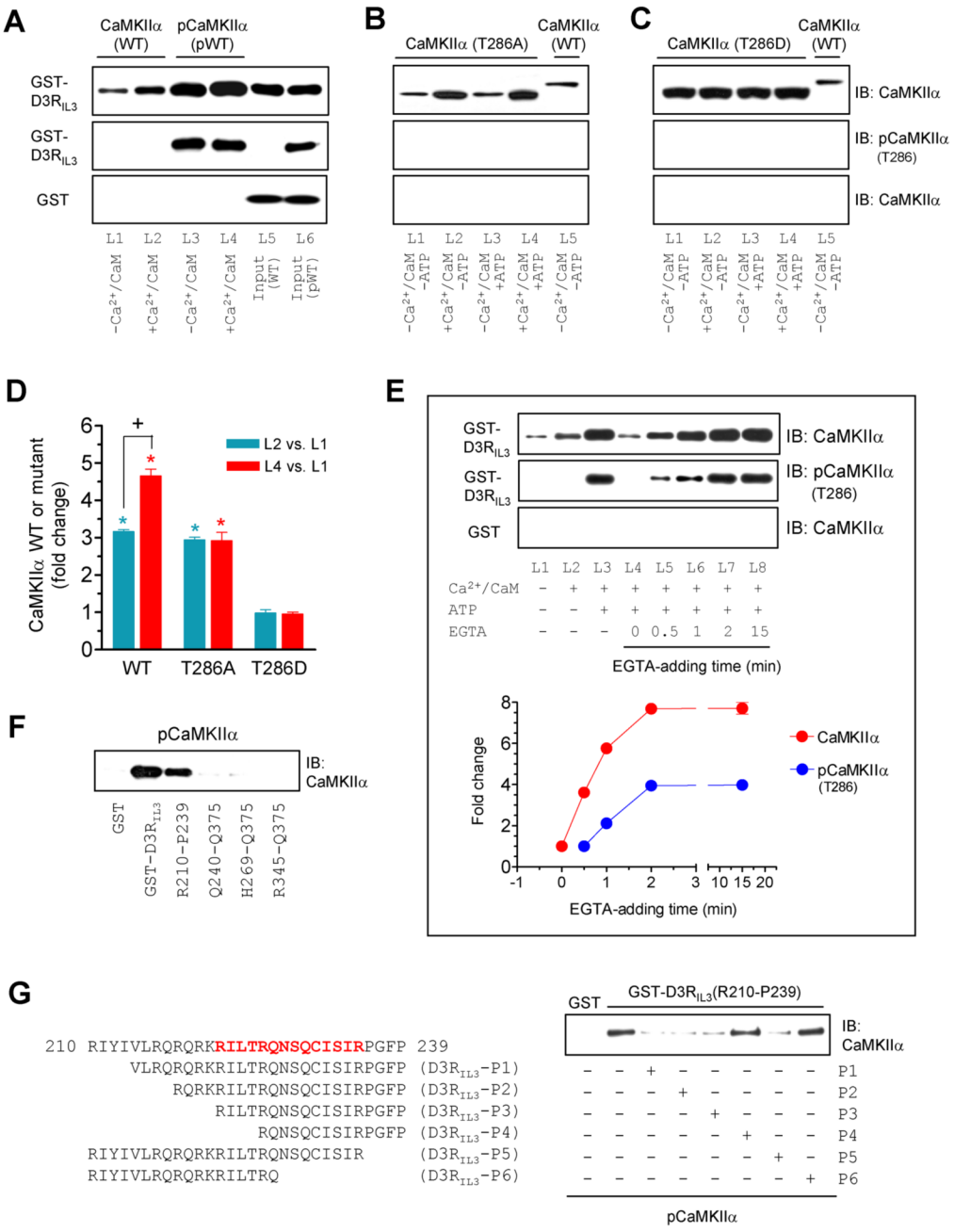

Figure 3. Influence of T286 autophosphorylation on the CaMKIIα-D3R$_{IL3}$ binding

(A–C) Binding of WT CaMKIIα/pCaMKIIα (A), mutant T286A (B), or mutant T286D (C) to GST-D3R$_{IL3}$. **(D)** A graph of the data from A–C. Blue and red bars represent changes in lane 2 (L2) and lane 4 (L4), respectively, over lane 1 (L1). *p < 0.05 versus L1. +p < 0.05 versus L2. **(E)** Effects of EGTA added at different times on the CaMKIIα binding to GST-D3R$_{IL3}$. EGTA was added 0, 0.5, 1, 2, or 15 min after the onset of the binding reaction. Representative immunoblots are shown above the quantified data. **(F)** pCaMKIIα bound to GST-D3R$_{IL3}$ and the GST-D3R$_{IL3}$(R210-P239) fragment. **(G)** Effects of six peptides derived from the R210-P239 fragment on the binding of pCaMKIIα to GST-D3R$_{IL3}$(R210-P239). The first 30-amino acid sequence of D3R$_{IL3}$ is shown. Bold letters (in red) indicate the potential CaMKIIα binding motif. Binding assays were performed between His-tagged WT CaMKIIα (~57 kDa), WT

pCaMKIIα (~57 kDa), T286A mutant (~50 kDa), or T286D mutant (~50 kDa) proteins and immobilized GST-D3R_{IL3} or GST-D3R_{IL3}(R210-P239) in the presence or absence of $CaCl_2$ (0.5 mM), CaM (1 μM), ATP (50 μM), or EGTA (1 mM) as indicated. Bound CaMKIIα, pCaMKIIα, or mutants were visualized by immunoblots. Data are presented as means ± SEM for 4–6 experiments per group.

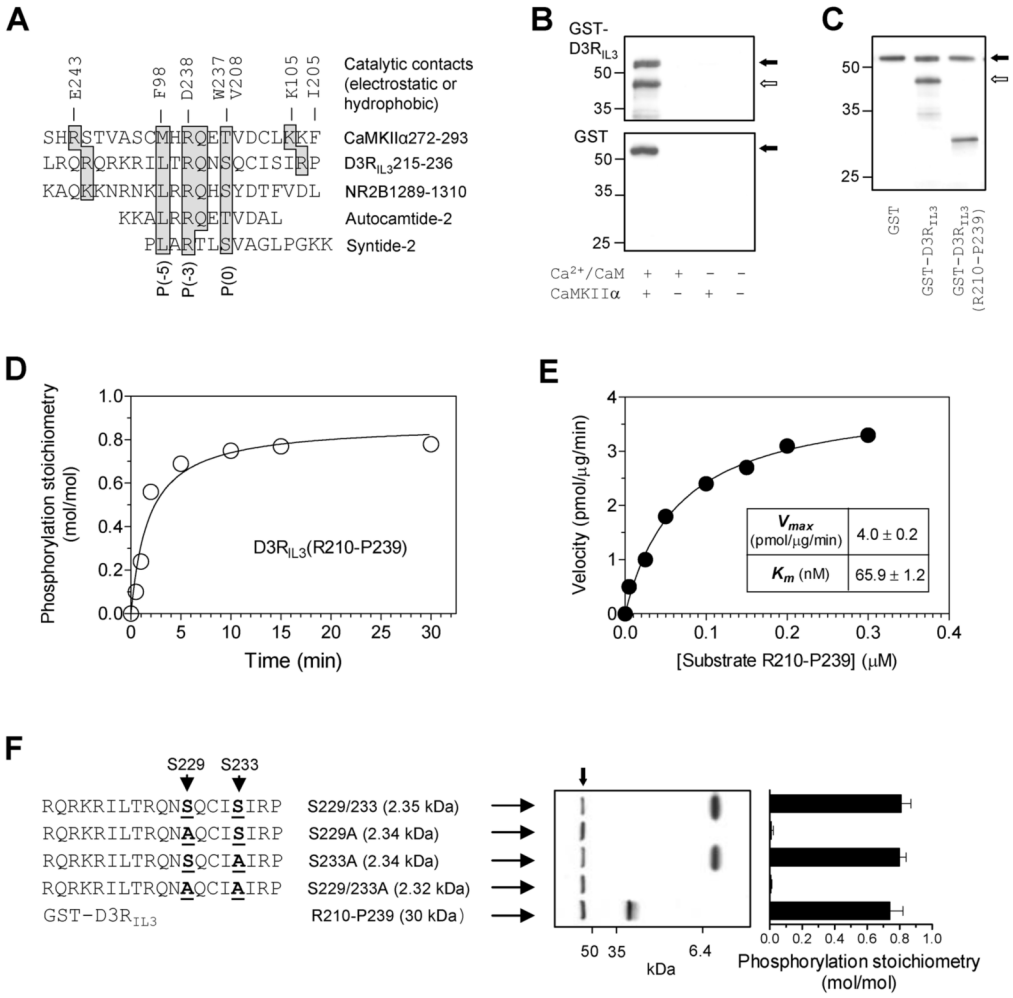

Figure 4. Phosphorylation of D3R$_{IL3}$ by CaMKII*α* *in vitro*

(A) Alignment of CaMKII phosphorylation sequences from different substrates. The key residues shaded in gray are contacted electrostatically or hydrophobically by the residues (E243, F98, D238, W237, V208, K105, and I205) from the catalytic domain of CaMKII. **(B)** Autoradiographs illustrating phosphorylation of GST-D3R$_{IL3}$ (upper) but not GST (lower) in the presence of Ca^{2+}/CaM. **(C)** An autoradiograph illustrating phosphorylation of GST-D3R$_{IL3}$ and GST-D3R$_{IL3}$(R210-P239). **(D)** Time course of D3R$_{IL3}$(R210-P239) phosphorylation. **(E)** Kinetic analysis of D3R$_{IL3}$(R210-P239) phosphorylation. The inset table shows the kinetic parameters. **(F)** Phosphorylation of synthetic peptides (WT or mutants). An autoradiograph shows phosphorylation of three peptides. Phosphorylation stoichiometry (means ± SEM) was calculated from the radioactivity measured on Coomassie-stained bands by liquid scintillation counting. Substrate proteins at 0.1 μM (B, C, D, and F) or increased concentrations (E) were incubated at 30°C for 1 min (E), 10 min (B, C, and F), or indicated times (D) with [γ-^{32}P]ATP and CaMKIIα in the presence of Ca^{2+} (0.5 mM)/CaM (1 μM) (C, D, E, and F) or as indicated (B). The solid arrows (B, C, and F) indicate autophosphorylated CaMKIIα whereas open arrows (B and C) indicate phosphorylated GST-D3R$_{IL3}$.

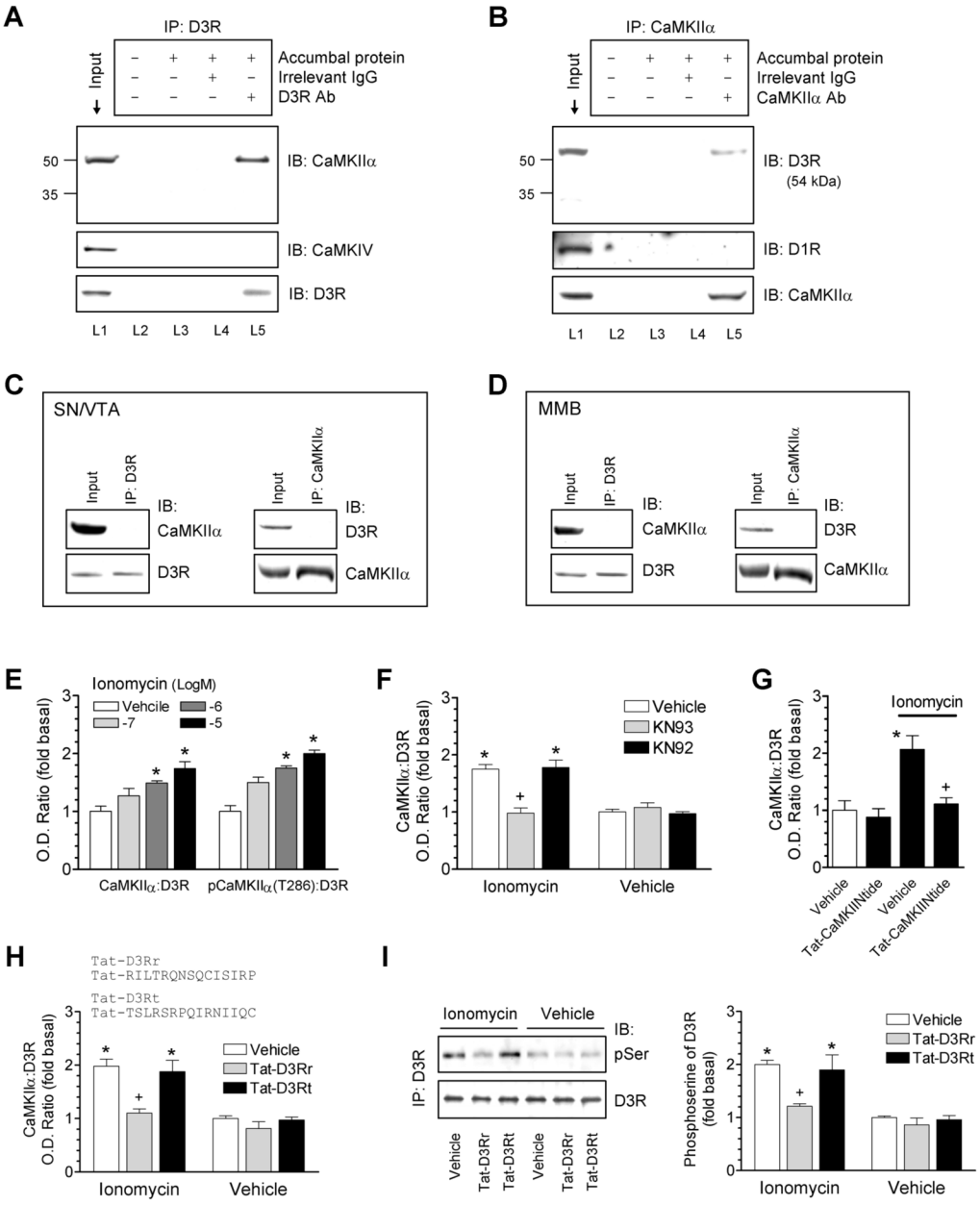

Figure 5. Association of CaMKIIα with D3Rs in accumbal neurons *in vivo*

(A and B) Coimmunoprecipitation (IP) of CaMKIIα and D3Rs in the synaptosomal fraction from the rat NAc. Lanes 3 and 4 showed no specific bands due to the lack of any antibody (L3) and the use of an irrelevant IgG (L4). **(C and D)** No coimmunoprecipitation of CaMKIIα and D3Rs was detected in the synaptosomal fraction from the rat substantia nigra (SN)/ventral tegmental area (VTA) and medial mammillary bodies (MMB). **(E)** Ionomycin (15 min) concentration-dependently increased the association of CaMKIIα and pCaMKIIα (T286) with D3Rs. **(F)** KN93 blocked the effect of ionomycin. Ionomycin (10 μM) was co-treated with KN93 or KN92 (20 μM) for 15 min. **(G)** Tat-CaMKIINtide blocked the effect of ionomycin. Tat-CaMKIINtide (5 μM) was applied 1 h prior to ionomycin (10 μM, 15 min). **(H)** Tat-D3Rr blocked the ionomycin-induced association of CaMKIIα with D3Rs. **(I)** Tat-D3Rr blocked the ionomycin-stimulated serine phosphorylation of D3Rs. Tat peptides (5-10 μM) were applied

1 h prior to ionomycin (10 μM, 15 min). Immunoblots (IB) of CaMKIIα, pCaMKIIα (T286), phosphoserine, or D3Rs were performed on D3R precipitates from drug-treated accumbal slices (E–G). Data are presented as means ± SEM for 3–5 experiments per group. *$p < 0.05$ versus vehicle or vehicle + vehicle. +$p < 0.05$ versus vehicle + ionomycin.

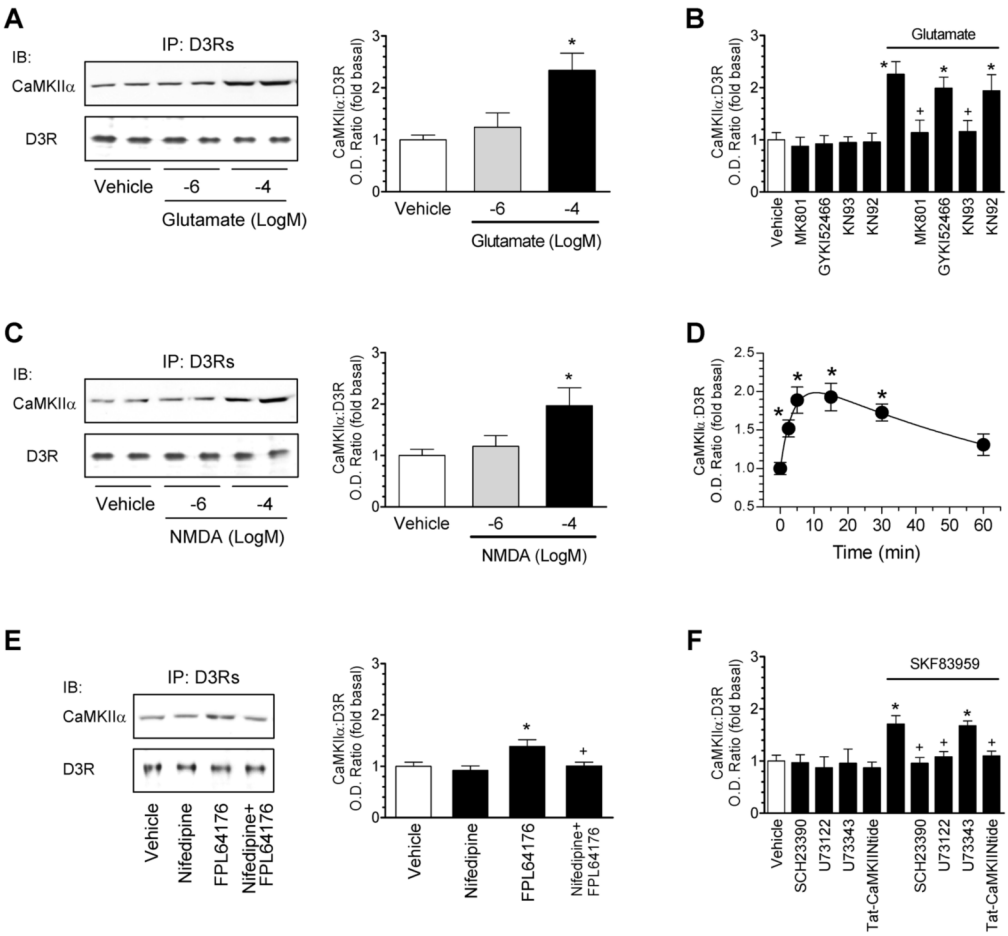

Figure 6. Regulation of CaMKIIα-D3R interactions by glutamate and dopamine receptors and VOCCs

(A) Glutamate increased the CaMKIIα-D3R interaction. **(B)** MK801 and KN93 but not GYKI52466 and KN92 blocked the CaMKIIα-D3R interaction induced by glutamate. **(C)** NMDA increased the CaMKIIα-D3R interaction. **(D)** The time course of the NMDA-stimulated CaMKIIα-D3R interaction. NMDA (100 μM/glycine 10 μM) was applied for 2.5, 5, 15, 30, or 60 min (D). **(E)** The VOCC activator FPL64176 induced a nifedipine-sensitive increase in the CaMKIIα-D3R interaction. **(F)** SKF83959 elevated the CaMKIIα-D3R interaction. Rat accumbal slices were treated with glutamate (1 or 100 μM/glycine 10 μM), NMDA (1 or 100 μM/glycine 10 μM), FPL64176 (20 μM), or SKF83959 (10 μM) alone or with MK801 (10 μM), GYKI52466 (10 μM), KN93 (20 μM), KN92 (20 μM), nifedipine (20 μM), SCH23390 (1 μM), U73122 (20 μM), or U73343 (20 μM) for 15 min. Tat-CaMKIINtide peptides (5μM) were applied 1 h prior to SKF83959 (10 μM, 15 min). Immunoblots (IB) of CaMKIIα or D3Rs were performed on D3R precipitates from drug-treated accumbal slices. Data are presented as means ± SEM for 4–5 experiments per group. *$p < 0.05$ versus vehicle or vehicle + vehicle. +$p < 0.05$ versus glutamate (B), FPL64176 (E), or SKF83959 (F).

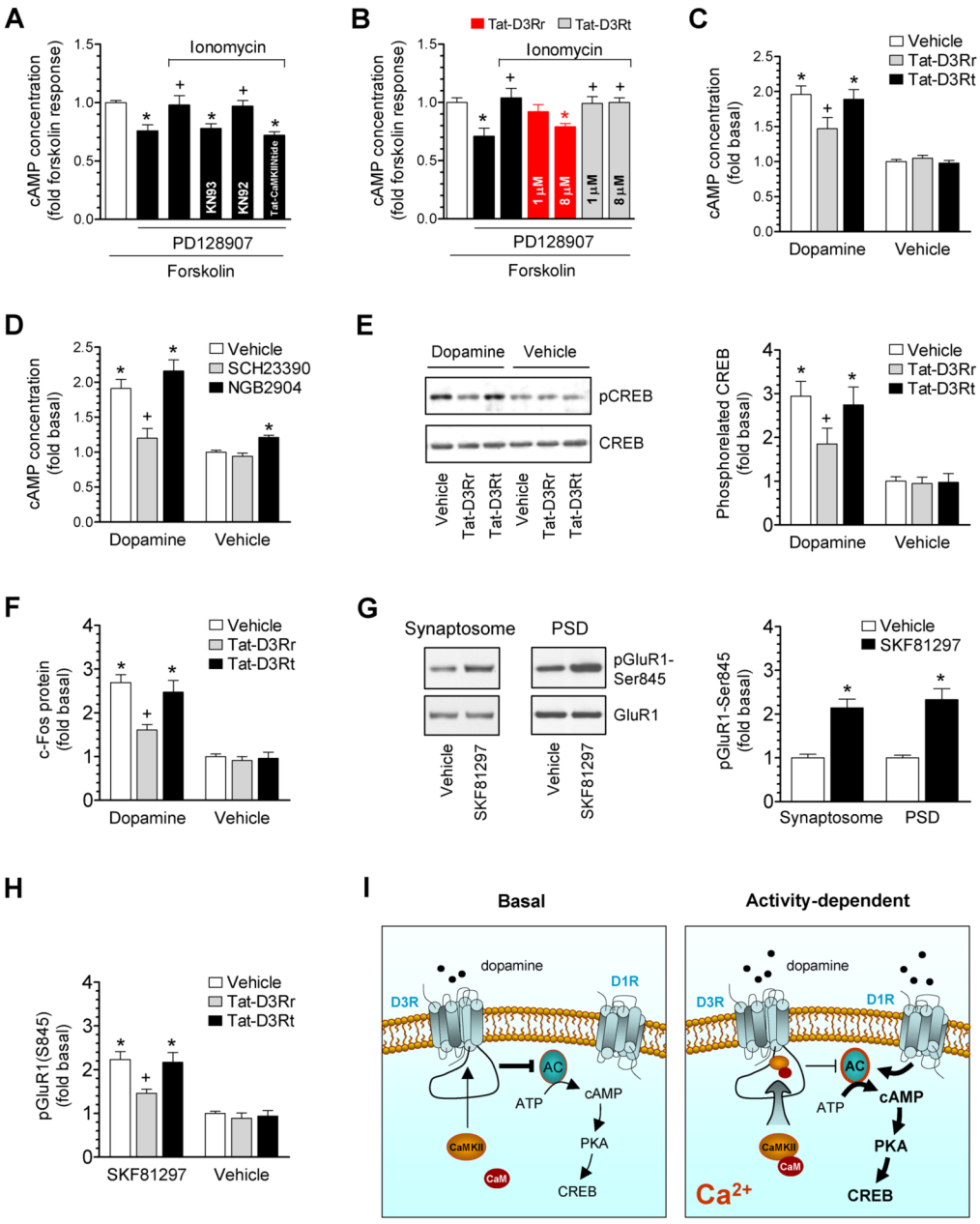

Figure 7. Inhibition of D3R function by CaMKII in rat accumbal slices

(A) Ionomycin antagonized the D3R-mediated inhibition of forskolin-stimulated cAMP accumulation. **(B)** Tat-D3Rr reversed the effect of ionomycin. **(C)** Effects of Tat-fusion peptides on dopamine-stimulated cAMP accumulation. **(D)** Effects of the D1R or D3R antagonist on dopamine-stimulated cAMP accumulation. **(E)** Effects of Tat-fusion peptides on dopamine-stimulated CREB phosphorylation. **(F)** Effects of Tat-fusion peptides on dopamine-stimulated c-Fos expression. **(G)** SKF81297 increased pGluR1-S845 levels. **(H)** Effects of Tat-fusion peptides on SKF81297-stimulated GluR1 phosphorylation. **(I)** A model of the Ca^{2+}-dependent regulation of D3Rs by CaMKII. AC, adenylyl cyclase. PD128907 (1–3 nM), ionomycin (10 μM with 1 mM $CaCl_2$), KN93 (20 μM), KN92 (20 μM), SCH23390 (1 μM), and/or NGB2904 (50 nM) were co-treated with forskolin (1 μM, 20 min) or dopamine (5 μM, 20 min) in A–D. In the experiments in which the Tat-fusion peptide (Tat-CaMKIINtide, Tat-

D3Rr, or Tat-D3Rt) was employed, the peptide at 5 μM (A), 1 and 8 μM (B), or 8 μM (C, E, F, and H) was applied 1 h prior to forskolin (A and B), dopamine (C, E, and F), or SKF81297 (H). SKF81297 was incubated at 10 μM for 5–10 min (G and H). Data are presented as means ± SEM for 5–7 experiments per group. *$p < 0.05$ versus forskolin alone (A and B), vehicle (G), or vehicle + vehicle (C–F and H). +$p < 0.05$ versus PD128907 + forskolin (A and B), vehicle + dopamine (C–F), or vehicle + SKF81297 (H).

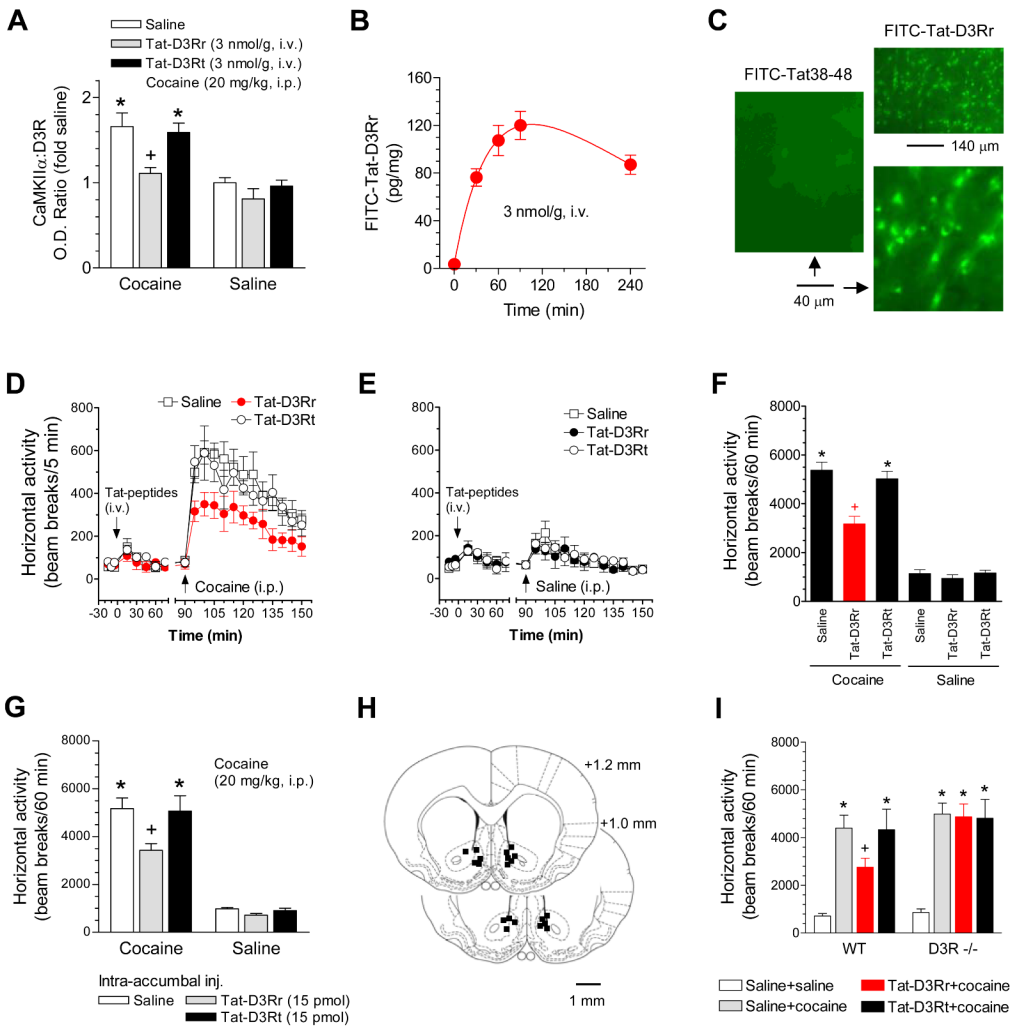

Figure 8. Disruption of CaMKIIα-D3R interactions altered cocaine-stimulated motor responses

(A) Effects of Tat-fusion peptides on the cocaine-stimulated CaMKIIα-D3R interaction. Rats were sacrificed 20 min after cocaine injection for conducting coimmunoprecipitation with the P2 fraction from the rat NAc. **(B)** Measurements of Tat-D3Rr concentrations in rat striatal tissue. Rats injected with FITC-Tat-D3Rr (3 nmol/g, i.v.) were sacrificed at indicated times. **(C)** Neuronal transduction of FITC-Tat-D3Rr but not FITC-Tat38–48 (3 nmol/g, i..v, 1.5 h) in the NAc shell region of rat accumbal sections. **(D and E)** Systemic Tat-D3Rr attenuated cocaine-stimulated locomotion (D) and had no effect on spontaneous motor activity (E). **(F)** A graph of the data from D and E obtained during 60 min after i.p. injection of drugs. **(G)** Intra-accumbal injection of Tat-D3Rr attenuated the cocaine-stimulated locomotion. **(H)** Location of microinjection sites within the NAc. Representative sites are illustrated on only one side for the bilateral injections of Tat-D3Rr (right) or Tat-D3Rt (left). **(I)** Tat-D3Rr attenuated the cocaine-stimulated locomotion in WT but not in D3R mutant mice. Cocaine (20 mg/kg, i.p.) was injected 60 or 90 min after an intra-accumbal injection (15 pmol/0.4 μl) or a systemic injection (3 nmol/g, i.v. for rats and 10 nmol/g, i.p. for mice) of Tat peptides, respectively. Data are presented as means ± SEM (n = 4–14 per group). *p < 0.05 versus saline + saline. +p < 0.05 versus saline + cocaine.